# PERFORMANCE OF ACID-TREATED ENDE NATURAL ZEOLITE IN ADSORPTION OF Ni(II) AND Co(II)

Nona Merry Merpati Mitan[1*], Sava Kamilah Zaldinur[1], Yulius Dala Ngapa[2], Nurul Aulia[1], Arie Sukma Jaya[3], and Yose Fachmi Buys[3]

[1] Chemistry Department, Faculty of Science and Computer Science, Universitas Pertamina, Jl. Teuku Nyak Arief, Simprug, Kebayoran Lama, Jakarta 12220

*nona.merry@universitaspertamina.ac.id

[2] Physics Education Department, Faculty of Teacher Training and Education, Universitas Flores, Jl. Sam Ratulangi Ende-Flores, Indonesia, 86319

[3] Mechanical Engineering Department, Faculty of Industrial Technology, Universitas Pertamina, Jl. Teuku Nyak Arief, Simprug, Kebayoran Lama, Jakarta, Indonesia 12220

**ABSTRAK**: Peningkatan pertumbuhan industri nikel dan kobal di Indonesia menimbulkan pengaruh ke berbagai aspek, termasuk aspek lingkungan. Limbah cair dari industri ini tentunya menuntut pengolahan yang tepat. Zeolit alam Ende digunakan sebagai material adsorben dalam menyerap ion nikel(II) dan kobal(II). Zeolit alam Ende diaktivasi menggunakan asam klorida 3 M. Karakterisasi zeolit dilakukan menggunakan X-Ray diffraction, Fourier Transform Infra Red, dan Semi Elektron Mikroskop.Hasil karakterisasi menunjukkan bahwa zeolit alam Ende utamanya tersusun dari mordenit dan klipnotilolite. Selanjutnya, zeolit alam Ende yang terakhir ini dimanfaatkan sebagai adsorben untuk larutan nikel(II) nitrat dan kobal(II) nitrat dengan konsentrasi masing-masing 0,15 M. Kinerja adsorpsi zeolit ditinjau dari variasi massa zeolit, variasi waktu kontak, variasi suhu, dan variasi konsentrasi. Dari berbagai variasi ini, zeolit alam Ende menunjukkan kinerja adsoprsi yang baik sebesar 0,60 g dalam mengadsorpsi ion nikel dan ion kobal. Variasi suhu menunjukkan bahwa pada suhu 70 $^{\circ}$C zeolit alam Ende menunjukkan efisiensi adsorpsi hingga 60 %. Hasil kajian ini menunjukkan bahwa zeolit alam Ende yang teraktivasi asam klorida mampu bertindak sebagai material adsorbent untuk ion nikel(II) dan ion kobal(II).

**Kata kunci**: Zeolit alam Ende; adsorpsi; ion nikel (II); ion kobalt (II); aktivasi asam..

**ABSTRACT**: The increasing growth of Indonesia's nickel and cobalt industry impacts various environmental aspects. Liquid waste from this industry certainly requires proper processing. Ende natural zeolite is an adsorbent material to adsorb nickel(II) and cobalt(II) ions. Ende natural zeolite is activated using 3 M of hydrochloric acid. Zeolite characterization was used X-ray diffraction, Fourier Transform Infra-Red, and Semi Electron Microscope. The characterization results show that Ende natural zeolite mainly comprises mordenite and clinoptilolite. Furthermore, the latter Ende natural zeolite is used as an adsorbent for nickel(II) and cobalt(II) solutions with concentrations of 0.15 M each. Zeolite adsorption performance is reviewed based on the variation of zeolite mass, variation of contact time, variation of temperature, and variation of concentration. From these variations, Ende natural zeolite shows good adsorption performance of 0.60 g in adsorbing nickel and cobalt ions. Temperature variations show that at a temperature of 70 $^{\circ}$C. Ende natural zeolite shows an adsorption efficiency of up to 60%. The results of this study indicate that Ende natural zeolite activated by hydrochloric acid can act as an adsorbent material for nickel(II) ions and cobalt(II) ions.

**Keywords**: Ende natural zeolite; adsorption; nickel(II) ion; cobalt(II) ion; acid activation.

# 1. INTRODUCTION

Nickel applications in industry are widely used because of its characteristics of resistance to corrosion, good electrical and thermal conductivity, and mechanical properties, so nickel has become a metal needed in new materials, new energy, information technology, aerospace, and other industries [1-3], likewise with cobalt [4].

As a result of the extensive use of nickel and cobalt, the impact of the waste produced is spread throughout the environment, both in water and soil [5-7 ].

Researchers have made many efforts to overcome nickel and cobalt contamination, for example, using deep eutectic solvents [8], nanocomposite derived from Sodium alginate/banana peels/reduced graphene oxide [9]. However, most materials used are neither cheap nor the manufacturing techniques. However, most materials used are neither cheap nor the manufacturing techniques. Therefore, zeolite is one of the materials used for the solution. Zeolite has been widely used in pollution solutions as an adsorbent material, for example, in ammonium adsorption [10], reduction in the sulfur content of gasoline models [11], hydrocarbon emission control in gasoline engines, [12], adsorption of carbon dioxide [13], wastewater from sugar factories and power plants [14]. Activation of natural zeolite Ende using magnetic composite to remove Cr(VI) metal from wastewater [15]. However, Ende natural zeolite has not been widely used to overcome nickel and cobalt waste contamination. Therefore, the current study examines the potential of acid-modified natural zeolite Ende as an adsorbent for nickel and cobalt ions to address the environmental problem of nickel and cobalt contamination.

# 2. EXPERIMENTAL METHOD
## 2.1 Materials and Apparatus

The materials in this research are Ende natural zeolite from Ende Regency, Flores, East Nusa Tenggara; cobalt(II) chloride hexahydrate (Merck, analytical grade); nickel(II) chloride hexahydrate (Merck, analytical grade); deionized water, and hydrochloride acid 37% (Mallinckrodt, analytical grade). The apparatus used in this research involved a ball mill (Horizontal Planetary Ball Mill, MSK-SFM-IS), incubator shaker (Biosan-Incubator ES-20/60), universal pH paper (MQuant), filter paper, analytical balance (Ohaus), 100 mesh sieve (Frame Mat'I S/STEEL), oven (Memmert GmbH & Co. KG, B120.0182), centrifuge (Eppendorf Centifuge 5430), Fourier Transform Infra-Red spectrophotmeter (FTIR, Thermo Scientific Nicolet iS5.ATR iD7), XRD (Olympus-BXT-534), Scanning Electron Microscope (SEM, Phenom XL G2 Desktop), UV-Vis Spectrophotometer (Thermo Scientific Genesys 10 S), and common glass apparatus.

## 2.2 Method

The procedures carried out in this research include sample preparation, sample activation, dye adsorption testing, sample characterization, and data analysis.

### 2.2.1 Zeolite Preparation and Activation

About 500 g of Ende natural zeolite was ground by ball mill to 100 mesh and washed with deionized water. Then, the zeolite was dried for 4 hours at a temperature of 110°C. Once dry, the zeolite was sieved again to ensure that the zeolite size remained the same after drying. Subsequently, the zeolite was ready for activation. The sample code for the Ende natural zeolite is natural zeolite (ZA), and the zeolite before activation or after washing is zeolite before activation (ZBA).

A total of 200 g of zeolite was prepared for the activation process. The sample activator used was 3 M hydrochloric acid. First, the zeolite was put into a 3 M HCl solution with a ratio of zeolite to 3 M HCl of 1:5, where every 50 g of zeolite was dissolved or activated with 250 mL of 3 M HCl solution. The mixture was then stirred using an incubator shaker for 3 hours at 200

rpm at 25 °C. Next, the zeolite was rinsed with deionized water until the pH of the zeolite returned to neutral. The neutralized zeolite was then dried for 4 hours at a temperature of 110 °C. After drying, the zeolite was filtered again using a 100-mesh sieve. The sample code for the HCl 3 M activated zeolite is zeolite after activation (ZAA).

## 2.2.2 Adsorption Performance

The procedure involves adsorption testing of Ni(II) and Co(II) metals with several parameters, including adsorbent mass, contact time, temperature, and concentration of each metal solution. This stage is the main stage that will produce experimental data to determine the maximum adsorption capacity, the adsorption isotherm model, and the comparison of optimum parameters on ZAA. The research procedure is as follows:

Ni(II) stock solution from nickel chloride hexahydrate with a concentration of 0.15 M as much as 100 mL. Likewise with the Co(II) stock solution from cobalt chloride hexahydrate with a concentration of 0.15 M as much as 100 mL.

### 2.2.2.1 Effect of Adsorbent Mass

The Ni(II) and Co(II) metal stock solutions with a concentration of 0.15 M were diluted to 0.1125 M, which was used as the test solution. Adsorbents with variations in mass of 0.2 g, 0.3 g, 0.4 g, 0.5 g, and 0.6 g were each added to 25 mL of Co and Ni solutions with a concentration of 0.1125 M. Then, the mixture was stirred using an incubator shaker for 1 hour at 200 rpm at 25 °C. After stirring, the solution was left to stand at room temperature for 15 minutes, centrifuged for 15 minutes at a speed of 3500 rpm, and then tested using a UV-Vis spectrophotometer. The adsorption test was carried out in triplicate.

### 2.2.2.2 Effect of Contact Time

The optimum mass obtained was added to 25 mL of Co and Ni solutions with a concentration of 0.1125 M. Then the mixture was shaken using an incubator shaker with varying times of 30, 60, 90, 120, and 180 minutes at 200 rpm. After shaking, the solution was left to stand at room temperature for 15 minutes, centrifuged for 15 minutes at a speed of 3500 rpm, and then tested using a UV-Vis spectrophotometer. The adsorption test was carried out in triplicate.

### 2.2.2.3 Effect of Temperature on Adsorption

The optimum mass obtained was added to 25 mL of Co and Ni solutions with a concentration of 0.1125 M. Then, the mixture was shaken using an incubator shaker at the optimum stirring time and a speed of 200 rpm, with varying temperatures of 30, 50, and 70 °C respectively. After shaking, the mixture was left to stand at room temperature for 15 minutes, centrifuged for 15 minutes at a speed of 3500 rpm, and then tested using a UV-Vis spectrophotometer. The adsorption test was carried out in triplicate.

### 2.2.2.4 Effect of Adsorbate Concentration on Adsorption

The optimum mass obtained was added to 25 mL of Co and Ni solutions with varying concentrations of 0.1125, 0.0975, 0.0825, 0.0675, and 0.0525 M, respectively. Then, the mixture was shaken using an incubator shaker at the optimum stirring time and a speed of 200 rpm at the optimum temperature. After shaking, the solution was left to stand at room temperature for 15 minutes, centrifuged for 15 minutes at a speed of 3500 rpm, and then tested using a UV-Vis spectrophotometer. The adsorption test was carried out in triplicate.

## 3. RESULTS AND DISCUSSION

### 3.1 Zeolite Characterization
### 3.1.1 X-Ray Diffraction (XRD) Characterization

The XRD was performed to characterize changes in the zeolite structure

before and after activation with 3 M hydrochloric acid. This characterization can be seen in Figure 1. There is no change in diffraction peaks between the zeolite before and after activation with 3 M HCl. This is because the zeolite structure has many metal oxides that allow it to maintain its original structure. The diffractogram results above indicate that this type of natural zeolite is a mixture of mordenite and clinoptilolite. This is based on the appearance of $2\theta$ angle peaks that match the characteristic peaks in the (JCPDS) data. The mordenite-type zeolite in this study is located at angles 29.59, 30.81, and 30.07°, respectively, while the clinoptilolite type appears at angles 15.49 and 24.06°. Ende natural zeolite is a mixed type of mordenite and clinoptilolite [16], with the highest intensity data appearing for mordenite-type zeolite at angles 25.63, 26.25, and 27.67° respectively. Meanwhile, the clinoptilolite type appears at angles 13.38, 22.36, and 29.07°, respectively.
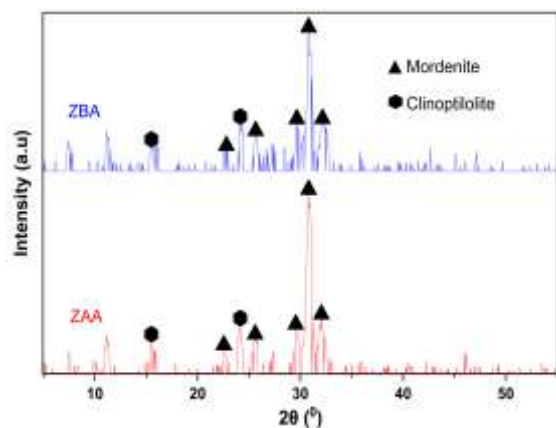


Figure 1. Difractogram of Ende natural zeolite

### 3.1.2 Fourier Transform Infra-Red (FTIR) Characterization

As seen in Fig. 2, the characterization of functional groups in ZAA is as follows. Activation with HCl on Ende natural zeolite focuses on removing surface impurities, expanding the surface area, and enlarging the pore size without changing its bonds. The region 786-693 cm$^{-1}$ is usually associated with the vibrational region of tetrahedral Si-O and Al-O. The region 1024-1000 cm$^{-1}$ is the region of asymmetric stretching vibrations of $TO_4$ bonds (T= Si and Al), interpreted from the absorption bands on the main structural units of zeolite [17].
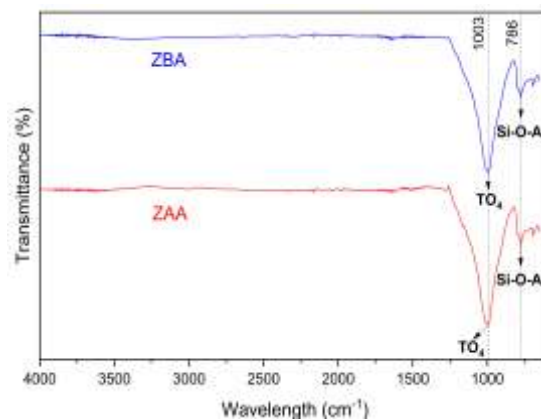


Figure 2. Spectra of ZBA and ZAA

### 3.1.3 Scanning Electron Microscope (SEM) Characterization

Characterization using an SEM was used to observe whether there are differences in the surface structure of Ende zeolite without activation and after activation with HCl 3 M. These differences can be seen in Fig. 3. The image shows the zeolite activated with HCl 3 M has more empty spaces (black areas) than before activation. These empty spaces indicate that the activated zeolite is smaller than the zeolite before activation. In addition, SEM characterization can also reveal the atomic concentration of both zeolites as shown in Table 1. The zeolite activated with HCl undergoes dealumination, indicated by the decrease in Al concentration from 9.12% to 5.12%. A low Si/Al ratio has high selectivity towards H+ and increases the acidity of the zeolite. The higher the acidity of an adsorbent, the more active sites the zeolite will have, and the more metal ions will be adsorbed. This is because H$^+$ will be exchanged with metal cations [18] as follow:

Zeolite-H$^+$ + Ni$^{2+}$ → Zeolite-Ni$^{2+}$ + H$^+$
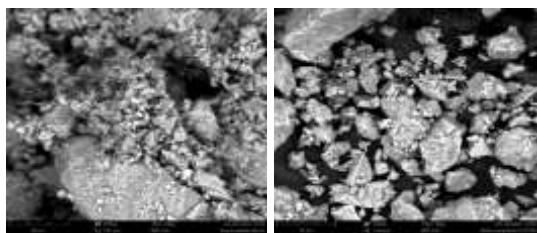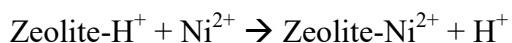


Figure 3. Morphology of a) ZBA and b) ZAA

Tabel 1. The concentration of atomic content in zeolite

| Zeolite | %Si | %O | %Al |
|---------|-------|-------|------|
| ZBA | 22.60 | 63.52 | 9.12 |
| ZAA | 19.60 | 73.52 | 5.15 |

## 3.2 Adsorption Performance of Ende Natural Zeolite

### 3.2.1 Effect of Adsorbent Mass on Adsorption

One of the adsorption tests involves varying the adsorbent mass to determine the optimal amount of adsorbent required for maximum adsorbate uptake. The test results are shown in Fig. 4. The figure demonstrates that the qe value decreases as the adsorbent mass increases. This is because when the adsorbent mass is small, the active sites on the zeolite surface do not function optimally in adsorption. Figure 4 shows that the adsorbent mass of 0.6 g is the most optimal in adsorbing Ni(II) and Co(II) ions. This is because 0.6 g represents the highest variation in adsorbent mass, leading to a more optimal ability to adsorb the nickel and cobalt from solutions.

This is related to the effect of activation, which causes impurities to be removed, making it easier for the adsorbent surface sites to interact with the adsorbate. Furthermore, from the variation in adsorbent mass, it is also possible to calculate the adsorption efficiency of the adsorbent towards Ni(II) and Co(II) metal ions. The calculation can use the formula as shown in Equation 1.

$$\text{Adsorption efficiency} = \frac{(Co - Ce)}{Co} \; x \; 100\% \quad (1)$$

ZAA can adsorp Ni(II) and Co(II) metals by 11 to 35%. The high adsorption efficiency values for Ni(II) and Co (II) metals in the ZAA sample are due to the influence of activation. Activation removes impurities in the sample, making the adsorbent high-purity [19]. High purity will optimize the absorption of Ni(II) and Co(II) metals. The trend of the adsorption efficiency graph can be seen in Fig. 5. Based on the figure, the optimum adsorbent mass is 0.6 g for both adsorption of Ni(II) and Co(II) metals ions.
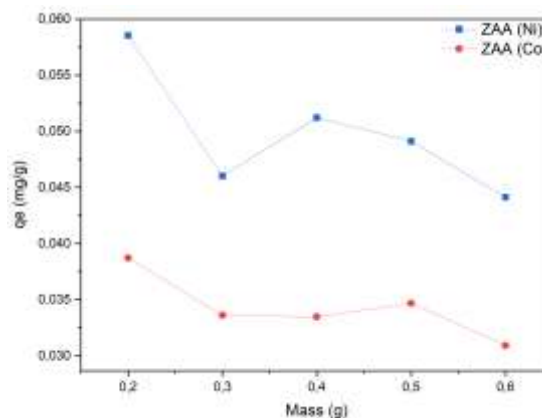


Figure 4. Adsorption capacity of ZAA in mass variation during adsorption of Ni(II) and Co(II)
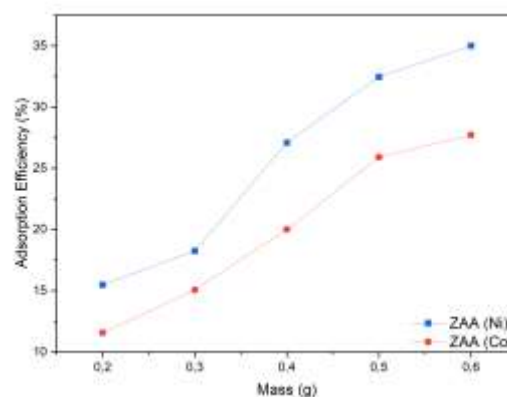


Figure 5. Effect of adsorbent mass on ddsorption efficiency of Ni(II) and Co(II) ions

### 3.2.2 Effect of Contact Time on Adsorption

Figures 6 and 7 show that the activated zeolite sample makes the zeolite characteristics free from impurities, so many active sites on the zeolite surface are empty, increasing the adsorption of the adsorbate. The optimum time for this adsorption is 180 minutes. This optimum time will become a fixed variable in subsequent adsorption tests. The efficiency at a contact time of 180 minutes is due to the effect of molecular collisions. The longer the contact time, the more molecular collisions.
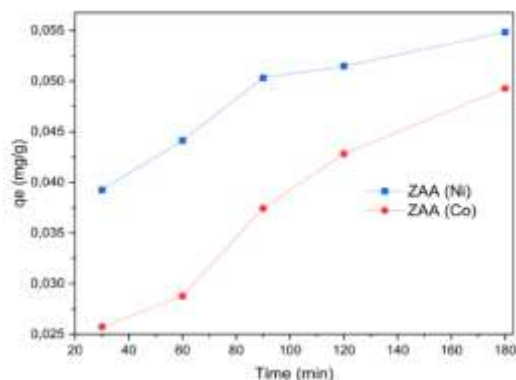


Figure 6. Adsorption capacity of ZAA in time variation during adsorption of Ni(II) and Co(II)
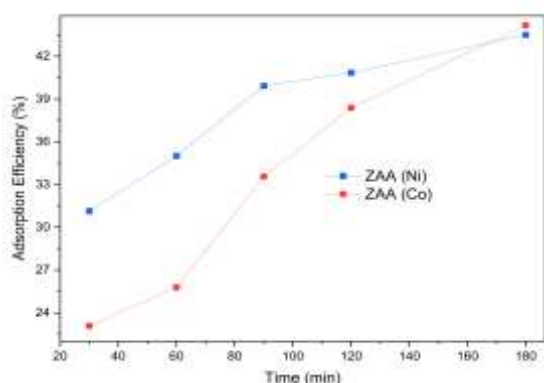


Figure 7. Adsorption efficiency of Ni(II) and Co(II) metal by ZAA versus contact time

Adsorption with varying contact times can also be used to determine the adsorption phenomenon, whether physisorption or chemisorption, by calculating the adsorption kinetics, namely pseudo-first-order and pseudo-second-order. Both orders can be calculated based on plotting between ln Ce versus time for the pseudo-first-order and 1/Ce versus time for the pseudo-second-order.
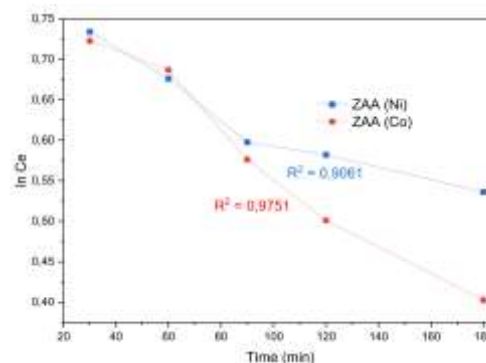


Figure 8. Plot pseudo first-order equation
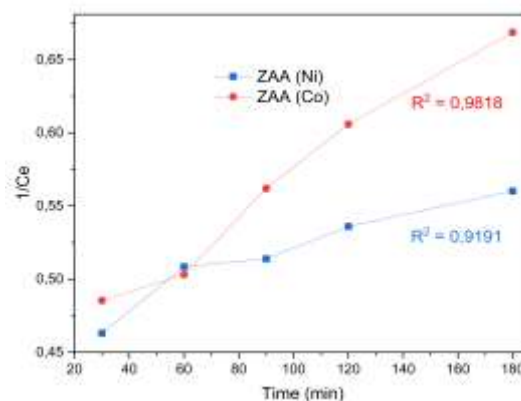


Figure 9. Plot of a pseudo-second-order equation

The calculation results are obtained by fitting the data into a linear equation, resulting in the rate constant value and the correlation coefficient value ($R^2$). The calculation results can be seen in Fig. 8 and 9. The highest $R^2$ values were obtained for the ZAA sample when adsorbing Ni(II) and Co (II) metals, namely $R^2 = 0.9442$ and $R^2 = 0.9816$, which are in the pseudo-second-order. The ZAA sample undergoes physisorption, which involves the formation of relatively weak chemical bonds between the adsorbate molecules on

the adsorbent. This type of multilayer adsorption involves van der Waals forces in its process, which causes the adsorption process to proceed slowly [20].

### 3.2.3 Effect of Temperature on Adsorption

Adsorption testing was also conducted with temperature variations to determine whether increasing the temperature would increase the zeolite's ability to adsorb metal ions. Figure 10 demonstrates the effect of temperature on the adsorption of Ni and Co metals by zeolite. It shows that as the temperature increases, the adsorption also increases. The increase in adsorption can be influenced by temperature, which is caused by changes in the kinetic energy of molecules.
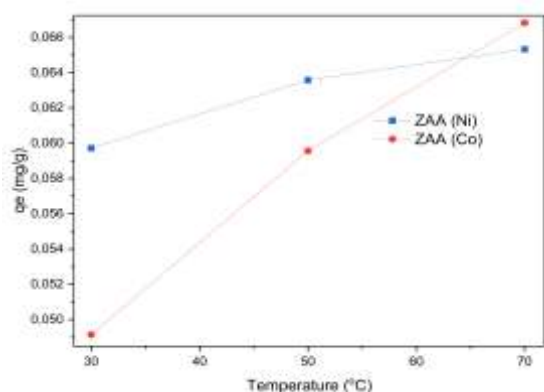


Figure 10. Adsorption capacity of ZAA in temperature variation during adsorption of Ni(II) and Co(II)

In this case, an increase in temperature will urge the metals to gain higher kinetic energy, leading to a faster diffusion process in the solid phase of the zeolite. Moreover, the increase in metal adsorption is also caused by an increase in the frequency of collisions between the zeolite sample and the metals. This will also affect the adsorption efficiency; the higher the temperature, the greater the percentage of adsorption efficiency. The calculation of adsorption efficiency can be done using Eq. 1. The adsorption of cobalt at high temperatures is observed to be greater than that of nickel. This is because density and viscosity depend on temperature. So, in increasing temperature, smaller density and viscosity values will result in higher diffusivity [21]. As it is known that cobalt has a lower density and viscosity compared to nickel, the adsorption of cobalt is greater than that of nickel.

### 3.2.4 Adsorption Isotherm

Adsorption testing through variations of the metal solution concentration can be used to determine the adsorption capacity value at (Qe). The Qe value is obtained from the calculation results of the adsorption isotherm on the Langmuir model. The adsorption isotherm has two very common models, namely Langmuir and Freundlich. The Langmuir model isotherm represents the adsorption process occurring at uniform or homogeneous active sites. In the Freundlich model, the adsorption process occurs on a heterogeneous or multilayer adsorbent surface and usually occurs physically. The following equations are applied for the determination of the Langmuir and Freundlich models:

$$\frac{Ce}{Qe} = \frac{1}{K_L.Qm} + \frac{1}{Qm} Ce \qquad (2)$$

$$log \ Qe = log \ K_f + \frac{1}{n} Ce \qquad (3)$$

The adsorption isotherm graph can be seen in Fig. 12. The graph shows a trend where increasing metal concentration decreases the zeolite's adsorption capacity. This is because, at low metal concentrations, many binding sites are available on the zeolite. However, as the metal concentration increases, the number of ions competing to bind to the available sites on the adsorbent also increases. This gradual increase leads to a buildup at the adsorbent sites, causing the adsorbent to become saturated over time, and thus reducing its adsorption capacity [22]. Based on the adsorption isotherm calculation results, the maximum

capacity value of each sample was obtained. The Qe value can be seen in Table 2. The table shows that the highest maximum capacity is obtained from the ZAA sample when adsorbing Co(II) metal, with a 125 mg/g value. Meanwhile, for ZAA, when adsorbing Ni(II) metal, the value is 89.285 mg/g.

Tabel 2. Adsorption Isotherm Parameters of Langmuir and Freundlich Models

| Parameter | | Nickel | Cobalt |
| | | ZAA | ZAA |
|---|---|---|---|
| Langmuir | Qe (mg/g) | 89.285 | 125.000 |
| | $K_L$ (L/mg) | 0.0112 | 0.0080 |
| | $R^2$ | 0.9930 | 0.9943 |
| Freundlich | $K_f$ | 5.5206 | 6.1879 |
| | n | 2.2114 | 1.7325 |
| | $R^2$ | 0.9864 | 0.9964 |

The $R^2$ results obtained, as shown in Table 2, indicate that the ZAA sample for the adsorption of both solutions falls into the Langmuir isotherm model or occurs in a monolayer, where the interaction of the adsorbate with the adsorbent only occurs with one molecule.

## 4. CONCLUSIONS

The FTIR results show IR spectra in the region of 786-693 cm$^{-1}$, which corresponds to the Si-O and Al-O bond region, and in the region of 1024-1000 cm$^{-1}$, which is the asymmetric stretching vibration region of T-O bonds in the $TO_4$ tetrahedra (T= Si and Al). The difraktogram indicates that the zeolite type is clinoptilolite and mordenite. The micrographs shows that the atomic concentration of Al decreased from 9.12% to 5.12%, indicating dealumination. The optimum conditions for Ni(II) and Co(II) adsorption were determined through several variations. The optimum adsorbent mass was 0.6 g with the highest efficiency of 35.006 %, with a contact time of 180 minutes, the efficiency value was 49.322 %, at the optimum temperature of 70 °C the

efficiency was 59.88 %, and the optimum concentration was 0.0525 M with an efficiency value of 70.23%. At the optimum mass variation of 0.6 g, Ni (II) metal adsorption with ZAA has an adsorption efficiency of 35.0 %.

## 5. ACKNOWLEDGMENT

## 6. DAFTAR PUSTAKA

[1] Su C, Geng Y, Liu G, Borrion A, Liang J. 2024. Emergy-based environmental accounting of China's nickel production. *Ecological Indicators*, 161:112006.

[2] Sun H, Wu X, Wang X, Liu J, He G. 2024. End-of-life nickel recycling: Energy security and circular economy development. *Resources Policy,* 98:105308.

[3] Phadke R. 2024. Green nickel, electric vehicles and mining governance challenges in the U.S. *The Extractive Industries and Society,* 18: 101469

[4] Liu D, Wang X, Chen Y, Zhang B, Zhou J, Liu H. 2024. Cobalt distribution and its relationship with bedrocks and cobalt mineralizations in China. *Ore Geology Reviews*, 167; 105992

[5] Xiang Y, Lan J, Dong Y, Zhou M, Hou H, Huang BT. 2024. Pollution control performance of solidified nickel-cobalt tailings on site: Bioavailability of heavy metals and microbial response. *Journal* of *Hazardous Materrials*, 471:134295

[6] Kim KH, Shon ZH, Mauulida PT, Song SK. 2014. Long-term monitoring of airborne nickel (Ni) pollution in association with some potential source processes in the urban environment. *Chemosphere*, 111: 312–319.

[7] Zhao F, Huang Y, Wei H, Wang M. 2024. Ocean acidification alleviated nickel toxicity to a marine copepod under multigenerational scenarios but at a cost with a loss of transcriptome plasticity during recovery. *Science of The Total Environment*, 942: 173585

[8] Liu H, Xue K, Zhu W, Fan D, Dong Z, Wang, Y. 2024. Cobalt recovery from lithium battery leachate using hydrophobic deep eutectic solvents: Performance and mechanism. *Process Safety and Environmental Protection*, 190:1–10.

[9] Ali Z, Shoaib M, Ul-Haq N, Ahmed S, Younas U, Ali F, et al. Sodium alginate/banana peels/reduced graphene oxide nanocomposite beads for effective removal of copper and nickel from aqueous solutions. *Journal of the Indian Chemical Society,* 101(10): 101325.

[10] Fu H, Zhong L, Yu Z, Liu W, Abdel-Fatah MA, Li J. 2022. Enhanced adsorptive removal of ammonium on the Na+/Al3+ enriched natural zeolite. *Seperation and Purification Technology*, 298: 121507

[11] Dashtpeyma G, Shabanian SR, Ahmadpour J, Nikzad M. 2022. Effect of desilication of NaY zeolite on sulfur content reduction of gasoline model in presence of toluene and cyclohexene. *Chemical Engineering Research and Design*, 178:523–539.

[12] Feng C, Deng Y, E J, Han D, Tan Y, Luo X. 2022. Effects of the ZSM-5 zeolites on hydrocarbon emission control of gasoline engine under cold start. *Energy*, 260: 124924

[13] Choi HJ, Hong SB. 2022. Effect of framework Si/Al ratio on the mechanism of CO2 adsorption on the small-pore zeolite gismondine. *Chemical Engineering Journal* 433: 133800.

[14] Jangkorn S, Youngme S, Praipipat P. 2022. Comparative lead adsorptions in synthetic wastewater by synthesized zeolite A of recycled industrial wastes from sugar factory and power plant. *Heliyon*, 8: e09323.

[15] Neolaka YAB, Lawa Y, Naat J, Riwu AAP, Mango AW, Darmokoesoemo H. 2022. Efficiency of activated natural zeolite-based magnetic composite (ANZ-Fe3O4) as a novel adsorbent for removal of Cr(VI) from wastewater. *Journal of Materials Research and Technology*, 18: 2896–2909.

[16] Ngapa YD. 2017. Study of The Acid-Base Effect on Zeolite Activation and Its Characterization as Adsorbent of Methylene Blue Dye. *JKPK (Jurnal Kimia dan Pendidikan Kimia)*, 2(2): 90 – 96

[17] Gerawork M, Ayalew A, Moges D. 2019. Adsorption of Ni2+ and Cd2+ from Aqueous Solution by Using Natural Zeolites. *International Journal of Chemical Sciences Research* 17(2): 310

[18] Munthali M, Elsheikh M, Johan E, Matsue N. 2014. Proton Adsorption Selectivity of Zeolites in Aqueous Media: Effect of Si/Al Ratio of Zeolites. *Molecule,* 19 (12): 20468–81.

[19] Abebe B, Murthy HCA, Amare E. 2018. Summary on Adsorption and Photocatalysis for Pollutant Remediation: Mini Review. *Journal of Encapsulation and Adsorption Sciences*, 08(04):225–255.

[20] Králik M. 2014. Adsorption, chemisorption, and catalysis. *Chemical Papers,* 68(12):1625–1638.

[21] Manirethan V, Raval K, Rajan R, Thaira H, Balakrishnan RM. 2018. Kinetic and thermodynamic studies on the adsorption of heavy metals from aqueous solution by melanin nanopigment obtained from marine source: Pseudomonas stutzeri. *Journal of Environmental Management*, 214: 315–324

[22] Yoesoef A dan Rosariawari F. 2018. Penggunaan zeolite alam untuk adsorpsi ion Fe (II) dalam air tanah dengan aktivasi asam nitrat. *JURNAL ENVIROTEK*, 9(2)